

# Immunosuppressive activity is attenuated by *Astragalus polysaccharides* through remodeling the gut microenvironment in melanoma mice

Guiqing Ding  | Qianyi Gong | Jinyun Ma | Xiaojun Liu | Yuanhua Wang | Xiaodong Cheng

Institute of Clinical Immunology, Yueyang Hospital of Integrative Medicine, Shanghai University of Traditional Chinese Medicine, Shanghai, China

## Correspondence

Xiaodong Cheng, Institute of Clinical Immunology, Yueyang Hospital of Integrative Medicine, Shanghai University of Traditional Chinese Medicine, Shanghai 200437, China.

Email: xdcheng\_8@yeah.net

## Funding information

The Shanghai Science and Technology Action Innovation Plan (Grant/Award Number: No. 19401901600), the National Natural Science Foundation of China (Grant/Award Number No. 81973543), and the Education and Scientific Research Projects of 2021 in the 14th Five Year Plan of National Higher Education of Traditional Chinese Medicine (Grant/Award Number No. YB-20-08).

## Abstract

*Astragalus polysaccharides* (APS), the main effective component of *Astragalus membranaceus*, can inhibit tumor growth, but the underlying mechanisms remain unclear. Previous studies have suggested that APS can regulate the gut microenvironment, including the gut microbiota and fecal metabolites. In this work, our results showed that APS could control tumor growth in melanoma-bearing mice. It could reduce the number of myeloid-derived suppressor cells (MDSC), as well as the expression of MDSC-related molecule Arg-1 and cytokines IL-10 and TGF- $\beta$ , so that CD8<sup>+</sup> T cells could kill tumor cells more effectively. However, while APS were administered with an antibiotic cocktail (ABX), MDSC could not be reduced, and the growth rate of tumors was accelerated. Consistent with the changes in MDSC, the serum levels of IL-6 and IL-1 $\beta$  were lowest in the APS group. Meanwhile, we found that fecal suspension from mice in the APS group could also reduce the number of MDSC in tumor tissues. These results revealed that APS regulated the immune function in tumor-bearing mice through remodeling the gut microbiota. Next, we focused on the results of 16S rRNA, which showed that APS significantly regulated most microorganisms, such as *Bifidobacterium pseudolongum*, *Lactobacillus johnsonii* and *Lactobacillus*. According to the Spearman analysis, the changes in abundance of these microorganisms were related to the increase of metabolites like glutamate and creatine, which could control tumor growth. The present study demonstrates that APS attenuate the immunosuppressive activity of MDSC in melanoma-bearing mice by remodeling the gut microbiota and fecal metabolites. Our findings reveal the therapeutic potential of APS to control tumor growth.

## KEYWORDS

*Astragalus polysaccharides*, gut microenvironment, immunosuppressive activity, melanoma, myeloid-derived suppressor cells

This is an open access article under the terms of the Creative Commons Attribution-NonCommercial-NoDerivs License, which permits use and distribution in any medium, provided the original work is properly cited, the use is non-commercial and no modifications or adaptations are made.

© 2021 The Authors. *Cancer Science* published by John Wiley & Sons Australia, Ltd on behalf of Japanese Cancer Association.

## 1 | INTRODUCTION

Globally, cancer is a major problem that seriously endangers human health.<sup>1</sup> Malignant melanoma is an invasive skin cancer that originates from melanocyte lineage cells. It is characterized by rapid progress, a high mortality rate and extremely poor prognosis.<sup>2</sup> Clinically, numerous treatment strategies, such as radiotherapy, chemotherapy, targeted therapy and immunotherapy, have been developed, but controlling tumor growth and metastasis remains challenging. Of all the factors, the immunosuppressive microenvironment is crucial in tumor progression.<sup>3</sup> The myeloid-derived suppressor cells (MDSC) have attracted the most research attention, because they can interfere with antitumor immunity in a variety of ways, including to weaken the tumor-killing effect of CD8<sup>+</sup> T cells.<sup>4</sup> MDSC are associated with poor prognosis in patients with melanoma.<sup>5</sup> Therefore, finding more effective treatment options to regulate the tumor immune microenvironment (TIME) is the goal of many researchers.

In recent years, increasing evidence has shown that the gut microenvironment is a major factor affecting the progression of and therapeutic effects on malignant tumors, including melanoma,<sup>6</sup> which has become a research hotspot. It is believed that the variety and composition of gut microbiota, as well as their metabolic function, interact with tumor progression.<sup>7</sup> Mixed feeding or fecal microbiota transplantation (FMT) strategies can affect tumor growth in mice from different feeding environments.<sup>8</sup> Antibiotics, which can disturb the gut microbiota, can also affect tumor progression and the efficacy of immune checkpoint inhibitors (ICI).<sup>9,10</sup> The effect of gut microbiota on tumor progression is often associated with the change of TIME. Gut microbiota is thought to influence the infiltration and function of immune cells, such as antigen presenting cells (APC), MDSC, and CD8<sup>+</sup> T cells.<sup>11-13</sup>

A growing number of studies have recognized that plant polysaccharides are natural flora regulators, and they can enhance systemic immune function by regulating gut microbiota.<sup>14-16</sup> *Astragalus polysaccharides* (APS), the main effective component of *Astragalus membranaceus*, can enhance immune function and inhibit tumor growth. Our previous study showed that APS could inhibit tumor growth in melanoma-bearing mice.<sup>17</sup> However, the underlying mechanism has yet to be further studied.

In this work, we investigated the change in the immunosuppressive activity in melanoma-bearing mice after APS administration. We examined the relationship between the effect of antitumor immunity and the regulation of gut microbiota. Furthermore, we analyzed the changes in gut microbiota and their metabolic function, and we evaluated the correlation between changes in gut microbiota and fecal metabolites.

## 2 | MATERIALS AND METHODS

### 2.1 | Cell cultures

The mouse melanoma cell line B16-F10 was purchased from the Cell Bank of the Chinese Academy of Sciences, Shanghai Branch. Cells

were cultured in a 5% CO<sub>2</sub> incubator at 37°C. RPMI 1640 medium (Gibco) was used in cell culturing, with 10% FBS (Gibco). Once the cell density reached 80%-90%, trypsin was used for cell passage.

### 2.2 | Animal models

C57BL/6 mice (male, approximately 20 g, 5-6 weeks) were raised in specific pathogen-free conditions (temperature of 25 ± 2°C, relative humidity of 45% ± 5%, and a 12-hour light/dark cycle). After 1 week of acclimation, approximately 5 × 10<sup>5</sup> cells were injected subcutaneously into the right axillary region of each mouse to establish tumor models. Tumors were collected before they reached 2.0 cm in diameter.<sup>18</sup> All animal experiments were carried out in accordance with the standards approved by the Animal Ethical Committee of Yueyang Hospital of Integrative Medicine.

### 2.3 | Antibiotic cocktail

In the antibiotic disturbance experiment, dysbiosis was induced 1 week prior to the tumor inoculation by gavaging a 200-μL antibiotic cocktail (ABX) each day, including vancomycin (500 mg/L), ampicillin (1 g/L), neomycin (1 g/L), and metronidazole (1 g/L; sigma).<sup>19</sup> The ABX was administered until the end of the experiment. For FMT, the ABX was administered 2 weeks prior to the tumor inoculation and continued for 1 week.

### 2.4 | *Astragalus polysaccharides* administration and fecal microbiota transplantation

The day after tumor inoculation, mice in APS and APS + ABX groups were given APS (Shanghai Yuanye Biotechnology) 200 mg/kg/d by oral administration for 2 weeks, and the same volume of PBS was used in the "Model" and ABX groups. FMT was performed as previously described.<sup>20</sup> Feces from Model and APS groups were collected and made into suspensions, and every 100 mg of feces was dissolved into 1 mL of sterile PBS; 200 μL of fresh fecal suspensions were provided daily and lasted for 18 days.

### 2.5 | 16S rRNA gene sequencing of the gut microbiota

Fresh feces were collected and immediately frozen at -80°C until 16S rRNA sequencing. Microbial community genomic DNA was extracted from the fecal samples using an EZNA Soil DNA Kit (Omega Bio-tek). The DNA concentration and purity were checked using a NanoDrop 2000 UV-Vis spectrophotometer (Thermo Scientific). The hypervariable region V3-V4 of the bacterial 16S rRNA gene was amplified by PCR with specific primer pairs 338F (5'-ACTCCTACGGGAGGCAGCAG-3') and 806R

(5'-GGACTACHVGGGTWTCTAAT-3'). The amplified PCR product was extracted and then purified using the AxyPrep DNA Gel Extraction Kit (Axygen Biosciences), according to the manufacturer's instructions, and further quantified using a Quantus Fluorometer (Promega). Purified amplicons were pooled in equimolar amounts and paired-end sequenced on an Illumina MiSeq PE300 platform (Illumina) using Majorbio Bio-Pharm Technology. The quality control and splicing of the original sequences were carried out, and the data was analyzed on the free online platform of the Majorbio I-Sanger Cloud Platform (www.i-sanger.com).

## 2.6 | Untargeted analysis of feces by liquid chromatography–mass spectrometry

A 50-mg fecal sample was immersed in 400- $\mu$ L cold extraction solution (4:1 methanol: water). The suspension was extracted after grinding and centrifugation. The QC sample was a mixture containing 20  $\mu$ L suspension from each single sample. The resulting supernatant and the QC sample were used to conduct metabolome profiling on UHPLC-QE (Thermo Fisher Scientific).

## 2.7 | Flow cytometry

To obtain single cells, the isolated tumor tissues were digested in a 37°C thermostatic remote box with 10 mL digestion medium including 1 g/L Collagenase Type IV, .02 g/L DNase I, and 1 g/L Neutral Protease (Worthington Biochemical). For intracellular cytokine staining, tumor infiltrating lymphocytes were isolated by 40%/70% percoll density centrifugation. Cells were incubated in RPMI-1640 medium supplemented with 10% FCS for 5 hours, with the stimulation of a leukocyte activation cocktail and with the protein transport inhibitor (Brefeldin A; 550 583, BD Pharmingen). Before staining intracellular cytokine, the cells were fixed and permeabilized using a transcription factor buffer set (562 574, BD Pharmingen). In the spleen, single cells were obtained directly by grinding. The following antibodies were used: fixable viability stain 780 (565 388), CD11b FITC M1/70 (557 396), Ms Ly-6G/Ly-6C PerCP-Cy5.5 RB6-8C5 (552 093), MS F4/80 PE TER-2342 (565 410), MS CD11c APC HL3 (550 261), Ms CD3e PerCP-Cy5.5 145-2C11 (551 163), and Ms CD8a PE 53-6.7 (553 032; BD Pharmingen). Cells were acquired using a BD FACSVerser Flow cytometer and a Cytoflex Flow cytometer, and FlowJo V10 software was used to analyze data.

## 2.8 | Gene expression analysis by quantitative RT-PCR

Total RNA was extracted from tumor tissues using TRIzol Reagent (Thermo Fisher Scientific). An iScript cDNA Synthesis Kit (BIO-RAD) was used to synthesize cDNA according to the manufacturer's instructions.

Quantification of gene expression was conducted using a QuantStudio 7 Flex real-time PCR system (Thermo Fisher Scientific) with iTaq Universal SYBR Green SuperMix (BIO-RAD). The following primers were used in this study: Arg-1 (forward\_5'-CTCCAAGCCAAAGTCCTTAGAG-3', reverse\_5'-AGGAGCTGTCATTAGGGACATC-3'), IL-10 (forward\_5'-GCTCTTACTGACTGGCATGAG-3', reverse\_5'-CGCAGCTCTAGGAGCATGTG-3'), TGF- $\beta$  (forward\_5'-CCAGATCCTGTCCAAACTAAGG-3', reverse\_5'-CTCTTTAGCATAGTAGTC CGCT-3'), GAPDH (forward\_5'-CAGGAGGCATTGCTGATGAT-3', reverse\_5'-GAAGGCTGGGG CTCA TTT-3'). Relative mRNA levels were calculated using the comparative  $2^{-\Delta\Delta Ct}$  method and the GAPDH mRNA level was used for normalization.

## 2.9 | Cytokine analysis of serum

The blood of tumor-bearing mice was collected on the 14th day after tumor inoculation. Serum was harvested after centrifuging at 900g for 20 minutes and kept at -80°C before use. The cytokines, including IL-6, IL-1 $\beta$ , TNF- $\alpha$ , and IL-10 (Multi Sciences), were quantified according to the manufacturer's protocol.

## 2.10 | Statistical analysis

All data were presented as mean  $\pm$  SD. The significance between two groups was measured using an unpaired Student's *t* test. One-way ANOVA with Tukey's multiple comparisons test was used for comparison for more than two groups. Microbial diversity and metabolic analysis were performed using the Majorbio I-Sanger Cloud Platform. Spearman's correlation was performed to identify correlation between microbial communities and specific metabolites. \**P* < .05 was considered statistically significant.

## 3 | RESULTS

### 3.1 | *Astragalus polysaccharides* attenuate the immunosuppressive activity of myeloid-derived suppressor cells in melanoma-bearing mice

After 14 days of APS administration, tumor weights were recorded to assess the antitumor effect of APS. We observed that the tumor blocks from the APS group were much lighter than those from the Model group (Figure 1A,B). Next, we examined the contents of myeloid cells in the spleen of mice. The flow cytometry showed that compared with the Model group, the number of dendritic cells increased in the APS group and the number of macrophages and MDSC decreased, but only MDSC changed significantly (Figure 1C-F). The mRNA expression of arginase-1 (Arg-1), interleukin-10 (IL-10), and transforming growth factor- $\beta$  (TGF- $\beta$ ) were decreased in tumor tissues in mice from the APS group (Figure 1G). These results indicated that APS could regulate the immune function in melanoma mice and inhibit tumor growth.

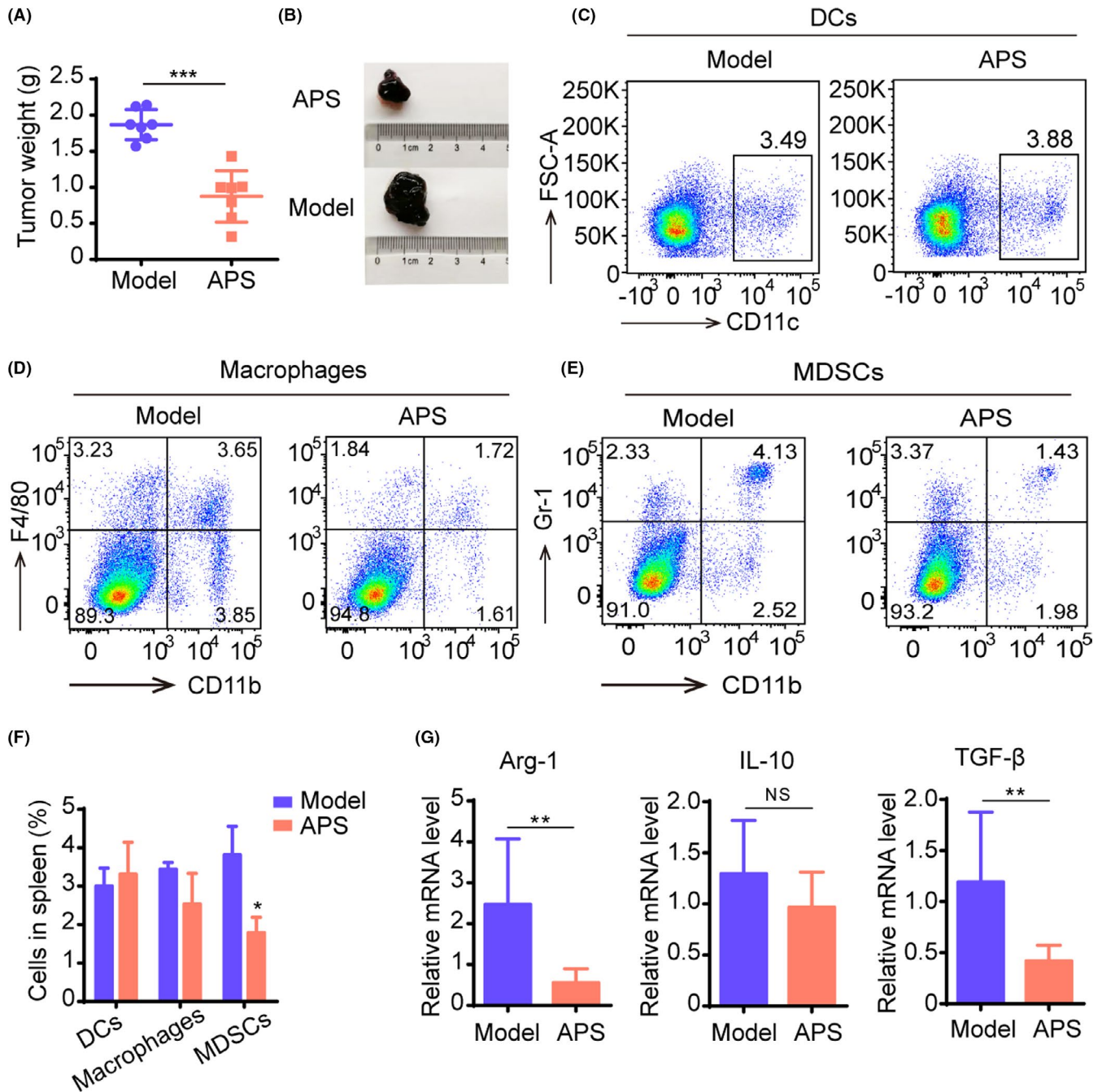


**FIGURE 1** *Astragalus polysaccharides* (APS) attenuate the immunosuppressive activity of myeloid-derived suppressor cells (MDSC) in melanoma mice. Mice were given APS (200 mg/kg/d) or normal saline (Model) after tumor inoculation. A, The tumor weight of mice from APS and Model groups. B, Image of tumor blocks. C–E, Changes of myeloid cells, including dendritic cells (DC) (C), macrophages (D), and MDSC (E) in the spleen of mice in the APS group compared with the Model group. F, Bar chart of DC, macrophages, and MDSC content in the spleen. (G), The expression of Arg-1, IL-10, TGF- $\beta$  was quantified by qRT-PCR. All these data were presented as mean  $\pm$  SD. \* $P < .05$ , \*\* $P < .01$ , \*\*\* $P < .001$

### 3.2 | *Astragalus polysaccharides* regulate immune function through remodeling the gut microbiota

An antibiotic cocktail was used to explore the influence of gut microbiota on tumor growth inhibition by APS. In melanoma-bearing mice models, the tumor volume was recorded from day 7 to day 14 after tumor inoculation. As shown in Figure 2A,B, the tumor

volume in the APS group increased slower than that in the Model group, while the treatment of APS combined with ABX weakened the antitumor effect of APS. On day 14, before tumors were collected, the tumor volume of the APS group was  $704 \pm 109.3 \text{ mm}^3$  versus  $1555.9 \pm 74.8 \text{ mm}^3$  in the Model group, and the tumor volume of the group treated with APS combined with ABX was  $1432.6 \pm 59.7 \text{ mm}^3$ .

Next, we investigated whether the immune function changed under the condition of ABX interference. The results showed that the number of MDSC in the APS group was the least among four groups, and no difference was seen between APS + ABX and Model groups (Figure 2C,D). MDSC are believed to exert an immunosuppressive effect mainly by inhibiting the proliferation and function of CD8<sup>+</sup> T cells; tumor growth follows. Therefore, we examined the content of CD8<sup>+</sup> T cells in tumor tissues with the use of flow cytometry. As shown in Figure 2E, the number of CD8<sup>+</sup> T cells in the APS group was much higher than that in the Model group, while the number of CD8<sup>+</sup> T cells in the APS + ABX group was not significantly increased. The CD8<sup>+</sup> T cells' secretion of IFN- $\gamma$  was enhanced in the APS group (Figure 2F). These results suggested that APS affected the immune function of melanoma-bearing mice by regulating the gut microbiota.

Consistent with the reduced abundance of MDSC in mice from the APS group, the expression level of the cytokines interleukin-1 $\beta$  (IL-1 $\beta$ ) and interleukin-6 (IL-6) were strikingly decreased in the serum of mice after APS administration, while the expression levels of tumor necrosis factor- $\alpha$  (TNF- $\alpha$ ) and IL-10 revealed no significant changes (Figure 2G). A high serum level of IL-1 $\beta$  was also found in the ABX group, which was previously reported to be associated with poor clinical outcome.<sup>5,21</sup>

To further confirm whether the gut microbiota regulation is necessary for APS to suppress tumor growth, we carried out an FMT experiment (Figure 3A). The results showed that the fecal suspension from the APS group could also control the tumor growth (Figure 3B,C). Moreover, compared with the Model group, a decrease of MDSC and an increase of CD8<sup>+</sup> T cells were found in tumor tissues from the A-FMT group (Figure 3D,E). Therefore, we hypothesized that APS reversed the TIME by regulating the gut microbiota.

### 3.3 | *Astragalus polysaccharides* regulate the composition of gut microbiota in melanoma mice

To understand the effect of APS on the gut microbiota in melanoma-bearing mice, we analyzed the diversity and composition of gut microbiota in the Model, APS, ABX and APS + ABX groups. First, the Shannon index and the Chao index were used to estimate the  $\alpha$ -diversity of gut microbiota in four groups. The results showed that there was no significant difference between Model and APS groups, although the  $\alpha$ -diversity of the ABX group and the APS + ABX group were significantly reduced (Figure 4A,B). Importantly, the composition of gut microbiota was significantly different in four groups. Principal coordinates analysis demonstrated that the microbial community structure was separated between Model and APS groups. They were different to the ABX group, while the combination of APS and ABX made the microbial community structure similar to that of the ABX group (Figure 4C). Furthermore, the differences in microbial composition among the four groups are clearly shown in the Venn diagram (Figure 4D).

We sought to determine which microorganisms were significantly different from the APS group and the Model group. At the species level, we observed that *Lactobacillus johnsonii*, *Faecalibaculum rodentium*, and unclassified\_g\_ *Lactobacillus* were enriched in the APS group, while *Sphingomonas leidyi*, *Bifidobacterium pseudolongum*, unclassified\_g\_norank\_f\_Christensenellaceae, and unclassified\_bacterium\_g\_Anaeroplasmata were downregulated (Figure 4E). Among all of them, the difference of *Bifidobacterium pseudolongum* was the most significant. Together, these results indicated that the regulation of gut microbiota was necessary for APS to exert its antitumor effect.

### 3.4 | *Astragalus polysaccharides* induce the changes of fecal metabolites through gut microbiota remodeling

We then performed untargeted metabolic analysis of feces by liquid chromatography-mass spectrometry in Model, APS, ABX, and APS + ABX groups. Through PLS-DA analysis, composition differences between Model and APS groups were obvious. Meanwhile, as ABX disrupted the regulation of gut microbiota composition by APS, fecal metabolites in the APS + ABX group were also similar to those in the ABX group (Figure 5A). The cluster heat map revealed that fecal metabolites in the Model and APS groups were well separated from each other; fecal metabolites were similar in ABX and APS + ABX groups (Figure 5B). As was evident in the volcano map, many metabolites had been upregulated or downregulated compared with the Model group (Figure 5C). These results suggested that gut microbiota regulated by APS altered the composition of fecal metabolites.

### 3.5 | *Astragalus polysaccharides* promote a shift in the metabolic function of the gut microbiota

Along with the composition changes of gut microbiota, their function changes substantially, which is reflected in the composition of metabolites. To clarify the influence of APS on metabolic function in melanoma-bearing mice, Kyoto Encyclopedia of Genes and Genomes (KEGG) pathway enrichment analysis was performed. The results showed that four biological pathways were significantly affected by APS compared with the Model group, and these changes were primarily linked to D-glutamine and D-glutamate metabolism, isoflavonoid biosynthesis, steroid biosynthesis, and arginine and proline metabolism (Figure 6A). Furthermore, these four biological pathways covered nine different metabolites, including L-glutamate, (R)-(+)-2-pyrrolidone-5-carboxylic acid, daidzein, 5-dehydroavenasterol, glycitein, genistein, 7-dehydrocholesterol 5,6-oxide, creatine, and 4-acetamidobutanoic acid (Figure 6B). We analyzed the abundance of these nine fecal metabolites in the four groups. From Figure 3B, it is evident that compared with the other three groups, glycitein and genistein were significantly downregulated in the APS group, while L-glutamate and creatine was upregulated in the APS group.

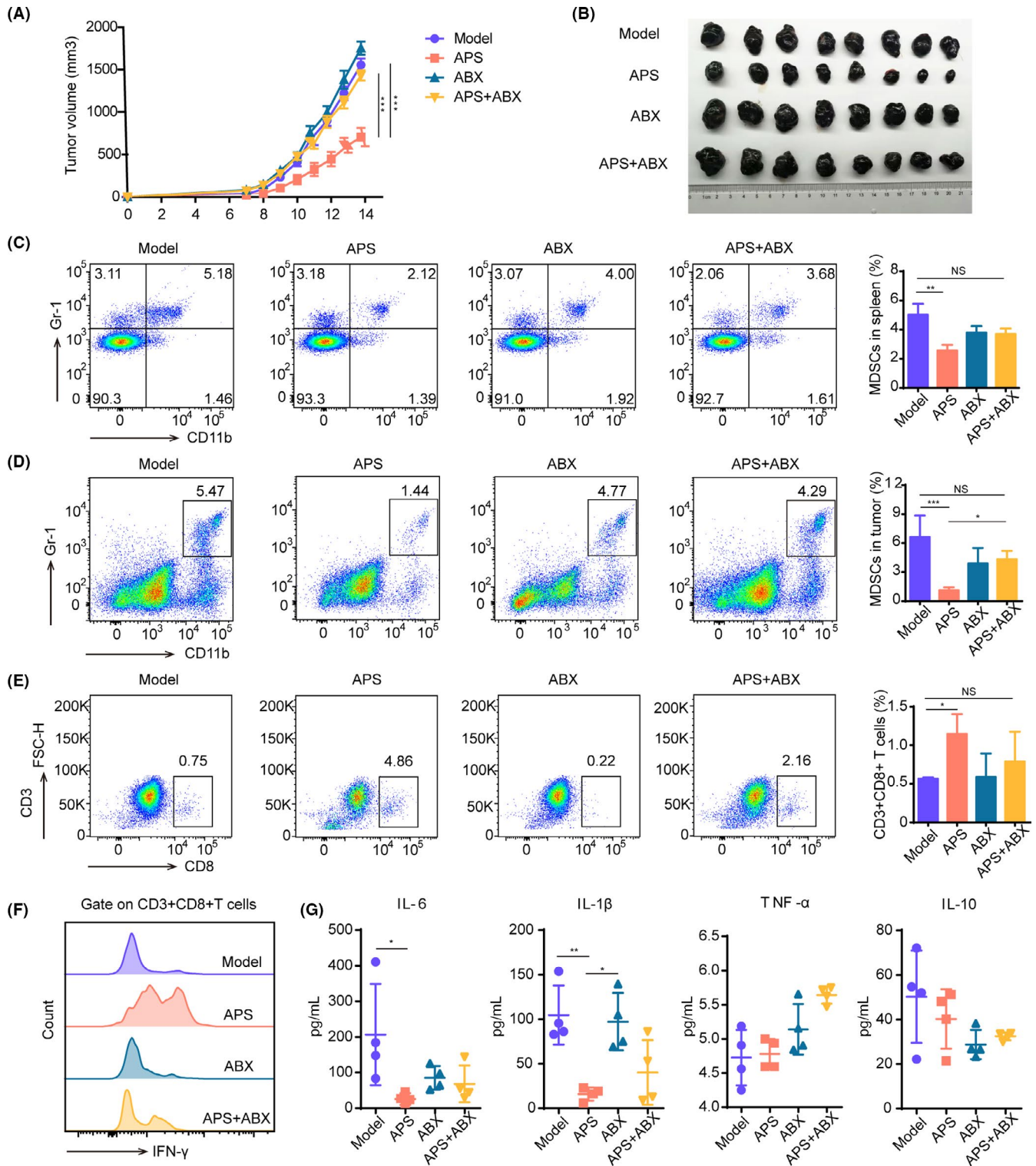


**FIGURE 2** *Astragalus polysaccharides* (APS) suppress tumor growth by modulating the gut microbiota in melanoma mice. A, Tumor volume changes in mice treated with APS (200 mg/kg/d), antibiotic cocktail (ABX) (200  $\mu$ L/d), APS + ABX or normal saline (Model) are shown. B, Image of tumor blocks collected from mice 14 d after tumor inoculation. C, D, The content of MDSC in the spleen (C) and tumor tissues (D). E, The content of CD8<sup>+</sup> T cells in tumor tissues. F, The expression of IFN- $\gamma$  on CD8<sup>+</sup> T cells in tumor tissues. G, inflammatory cytokines IL-6, IL-1 $\beta$ , TNF- $\alpha$ , and IL-10 in serum of mice. \* $P < .05$ , \*\* $P < .01$ , \*\*\* $P < .001$

The Spearman correlation analysis showed that the changes in creatine and L-glutamate were negatively correlated with *Bifidobacterium\_pseudolongum* and positively correlated with *Lactobacillus\_johnsonii*,

while the changes for glycitein and genistein were the opposite (Figure 7). Because previous studies have reported that L-glutamate and creatine are related to the antitumor effect, we postulated that the

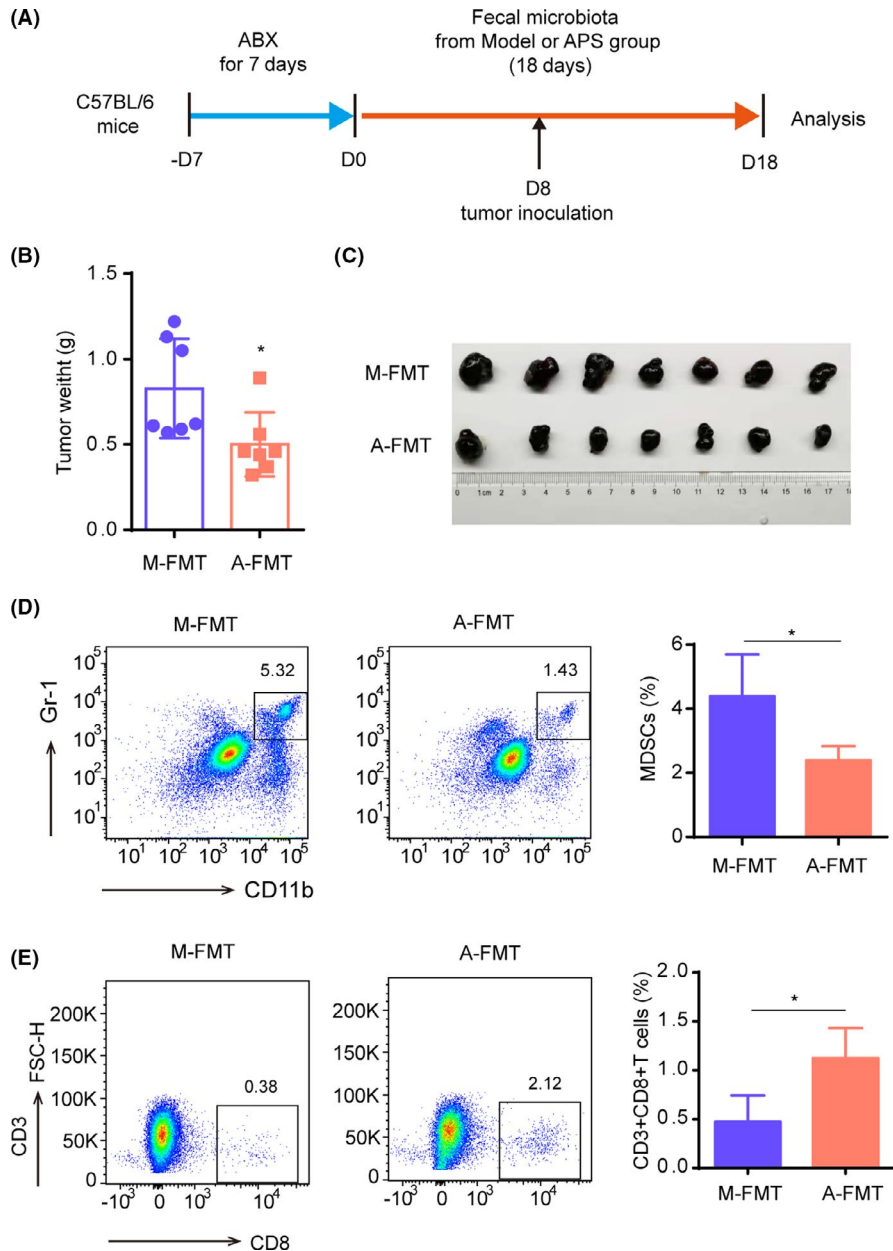


**FIGURE 3** Fecal suspension from the *Astragalus polysaccharides* (APS) group suppresses the tumor growth in melanoma mice. A, Flowchart of fecal microbiota transplantation (FMT) experiment. In the FMT experiment, the C57BL/6 mice received ABX 1 wk in advance, then mice were gavaged with fresh fecal suspension obtained from the Model group (M-FMT) or the APS group (A-FMT), respectively, until mice were killed. Tumor inoculation occurred on day 8 of fecal suspension administration. B, Tumor weight of mice from M-FMT and A-FMT groups. C, Image of tumor blocks. D, Contents of MDSC in tumor tissues of M-FMT and A-FMT groups. E, Contents of CD8<sup>+</sup> T cells in tumor tissues of M-FMT and A-FMT groups. \* $P < .05$

antitumor effect of APS was related to its regulation of gut microbiota composition and alteration of metabolic function.

## 4 | DISCUSSION

*Astragalus membranaceus* has been widely used to treat cancer and has demonstrated satisfactory therapeutic effects.<sup>22</sup> The composition of *Astragalus membranaceus* is relatively complex. APS, the main active component, have a variety of biological characteristics.<sup>23</sup> Data from in vivo and in vitro experimental studies have indicated that APS can control tumor growth in different types of tumor models.<sup>24</sup> Our previous research found that APS had the ability to control tumor growth in mice with melanoma,<sup>17</sup> but the exact mechanism remains unclear. Here, we confirmed the antitumor effect of APS and investigated the possible underlying mechanism.

In cancer, MDSC are heterogeneous cells that originate from myeloid cells, including immature dendritic cells and macrophages.<sup>25</sup> They are the main immunosuppressive cells in TIME and can lead to the promotion of tumor growth and metastasis.<sup>26</sup> In this study, we found that the number of MDSC and the mRNA expression of Arg-1, IL-10, and TGF- $\beta$  was reduced after APS administration. To some extent, this reflects the weakened ability of MDSC to inhibit CD8<sup>+</sup> T cells from killing tumor cells. Therefore, we speculated that APS attenuated the immunosuppressive activity of MDSC to suppress tumor growth.

The close relationship between gut microbiota and intestinal neoplasms, such as colorectal cancer, is beyond question.<sup>27</sup> Several reports have shown that the progression of parenteral tumors, such as melanoma, liver cancer and pancreatic cancer, are affected by gut microbiota.<sup>28,29</sup> The regulation of gut microbiota has become a new target for controlling parenteral tumor progression. It was found

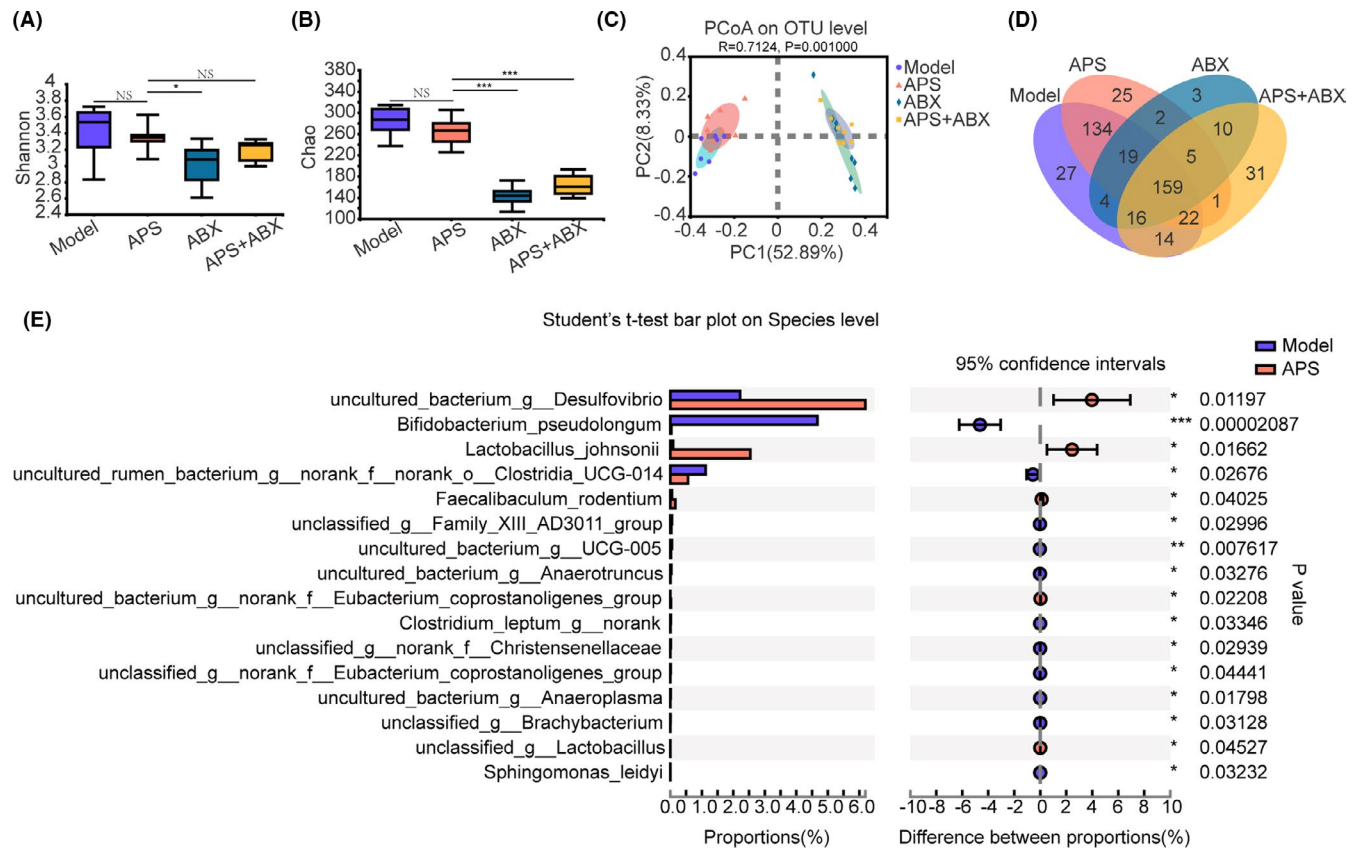


**FIGURE 4** *Astragalus polysaccharides* (APS) regulate the composition of gut microbiota in melanoma mice. The feces of mice from Model, APS, ABX, APS + ABX groups were collected to perform 16S rRNA gene sequencing. Shannon (A) and Chao (B) indexes were used to analyze  $\alpha$ -diversity of the gut microbiota. C, Principal coordinates analysis (PCoA) at the OTU level, in which the differences in groups can be seen from the distances between samples. D, Venn diagram of different microbial compositions in four groups. E, Bar plot of compositional differences at the species level in the gut microbiota of mice in the APS group vs the Model group using Student's *t*-test. \**P* < .05, \*\**P* < .01, \*\*\**P* < .001

in a sarcoma model mice that specific gut microbiota composition could amplify the content of extraintestinal MDSC and lead to tumor progression.<sup>5</sup> Gut microbiota can also affect the lung infiltration of MDSC in melanoma-bearing mice with a high fat diet and, finally, affect tumor metastasis.<sup>30</sup> Of interest, it was reported that APS were not easily directly absorbed by the intestine but they did regulate gut microbiota.<sup>14</sup> The current study found that APS had a therapeutic effect on acute colitis induced by sodium dextran sulfate and could restore the structure of gut microbiota.<sup>31</sup> They could also increase the level of 2-hydroxybutyric acid in the serum and liver of mice by regulating gut microbiota and improve lipid metabolism disorders in vivo and in vitro.<sup>32</sup> Therefore, we investigated whether the effect of the antitumor immunity of APS depended on the gut microbiota remodeling.

With the disturbance of gut microbiota by ABX, we found that the ability of APS to control tumor growth was weakened. The regulatory effects of APS on MDSC and CD8<sup>+</sup> T cells were also affected. Chronic inflammation leads to the production of immunosuppressive cells (like MDSC) and promotes tumor progression, while it has been reported that APS have an anti-inflammatory effect.<sup>33</sup> Therefore we examined the expression level of inflammatory cytokines in the serum of mice from Model, APS, ABX and APS+ABX

groups. In comparing the results of the Model and APS groups, we found that APS can, indeed, downregulate the expression of IL-6 and IL-1 $\beta$  in the serum of mice with melanoma but not TNF- $\alpha$ . An in vitro study also found that APS could reduce the expression level of pro-inflammatory genes except for TNF- $\alpha$ .<sup>34</sup> Moreover, we found that the expression level of IL-1 $\beta$  was high in the peripheral blood of mice treated with antibiotics. These mice had larger tumor volume and higher content of MDSC. This is consistent with reports that prolonged dysregulation of the gut microbiota caused by persistent antibiotic perturbation can trigger systemic inflammation.<sup>35</sup> In addition, we performed the FMT experiment and found that the fecal suspensions from APS interfered mice also had antitumor immunomodulatory effects. These results suggested that the changes in gut microbiota composition by APS might be related to the immune function regulation in mice with melanoma.

Next, we further investigated the influence of APS on gut microbiota in mice with melanoma. The remodeling of gut microbiota mainly includes changes in diversity and composition. Interestingly, no differences were found in  $\alpha$ -diversity between APS and Model groups based on the sequencing results of 16S rDNA, while there were differences in composition. After APS administration, most of the *Bifidobacterium\_pseudolongum* was significantly downregulated,

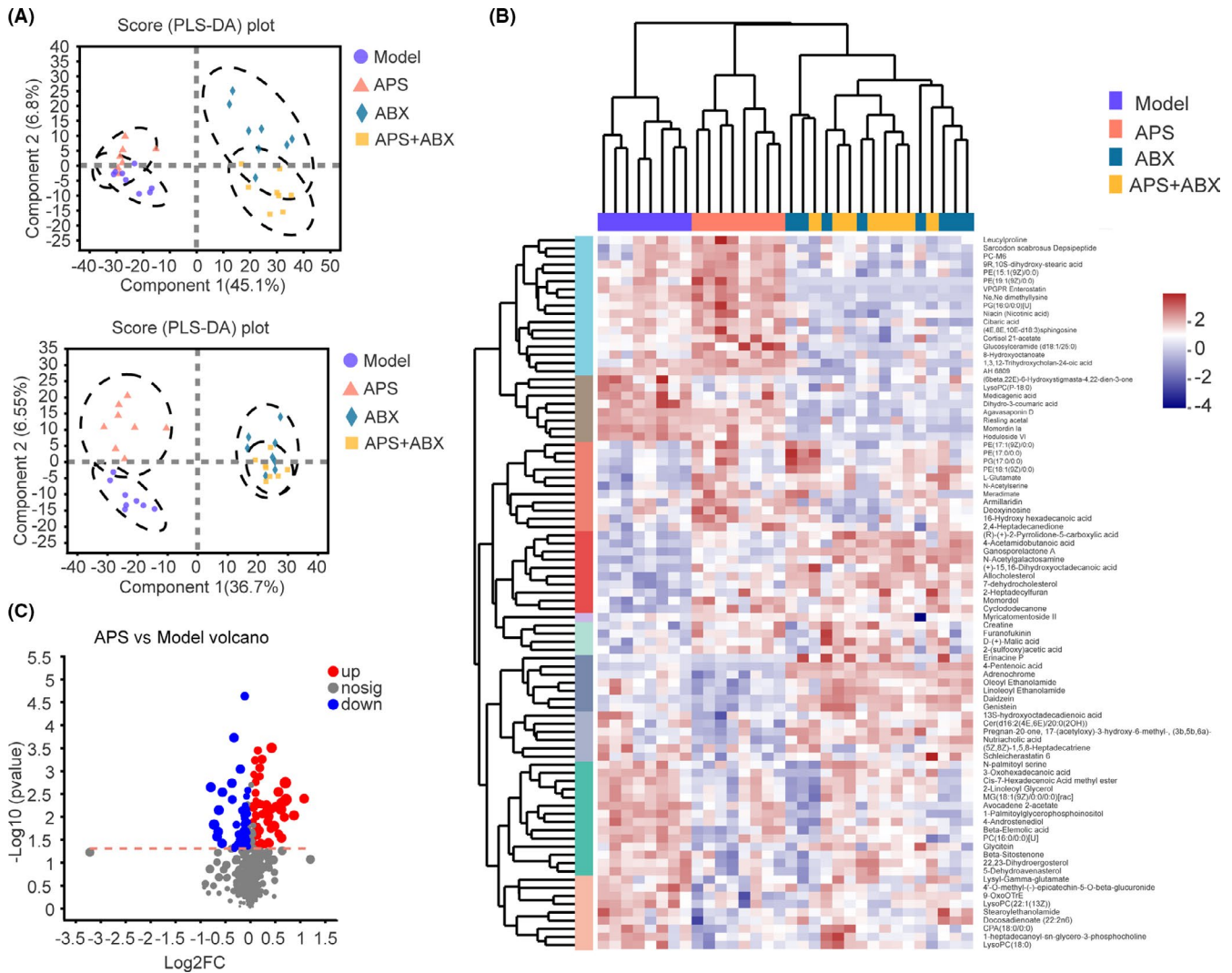


**FIGURE 5** The changes in gut microbiota by *Astragalus polysaccharides* (APS) influenced the fecal metabolites composition. A, PLS-DA plots of the fecal metabolites from all groups in the positive and negative ion modes. B, Cluster heat map showing relative abundances of metabolites at the genus level: from blue (less) to red (more). C, Volcano maps presenting metabolite expression changes in APS group vs Model group

whereas most of the *Lactobacillus* and *Lactobacillus\_johnsonii* was upregulated. Previous studies have shown that the abundance of *Bifidobacterium pseudolongum* is positively correlated with tumor progression, which can inhibit the activity of immune cells and promote the upregulation of the expression of factors related to tumor growth.<sup>36</sup> *Lactobacillus* and *Lactobacillus johnsonii*, as probiotics in the intestine, are important in maintaining host intestinal homeostasis and regulating host immune response.<sup>37</sup> *Lactobacillus* has been proved in several studies to have an antitumor effect,<sup>38,39</sup> and *Lactobacillus johnsonii* is also thought to enhance the efficacy of anti-CTLA4.<sup>40</sup> In addition, we found that APS was able to increase the abundance of *Faecalibaculum rodentium*, which could exert an antitumor effect in a mouse model of colorectal cancer by producing short-chain fatty acids, while *Holdemanella bififormis*, the bacteria corresponding to *Faecalibaculum rodentium* in the human body, could also inhibit tumor cell growth in vitro through release of short-chain fatty acids.<sup>41,42</sup> These results suggested that the changes in gut

microbiota composition by APS might be related to their antitumor effects.

Metabolites are one of the ways in which gut microbiota influence tumor progression.<sup>42-44</sup> In this study, we found that the composition of fecal metabolites in the APS group was different from that in the Model, ABX and APS + ABX groups. Further analysis showed that compared with the other three groups, metabolites L-glutamate and creatine were enriched in the APS group. It has been demonstrated that the supplementation of glutamate can inhibit tumor growth in breast cancer model mice.<sup>45</sup> Creatine could prevent skeletal muscle atrophy, weight loss, and tumor growth by attenuating the tumor-induced pro-inflammatory environment in rats.<sup>46-48</sup> In addition, combined use of creatine with ICI could continuously provide energy to T cells and, thus, more effectively combat cancer.<sup>49</sup> The Spearman correlation analysis also suggested that these metabolites might be involved in the antitumor effects of APS. Previous studies suggested that daidzein and genistein could exert antitumor effects.<sup>50,51</sup>

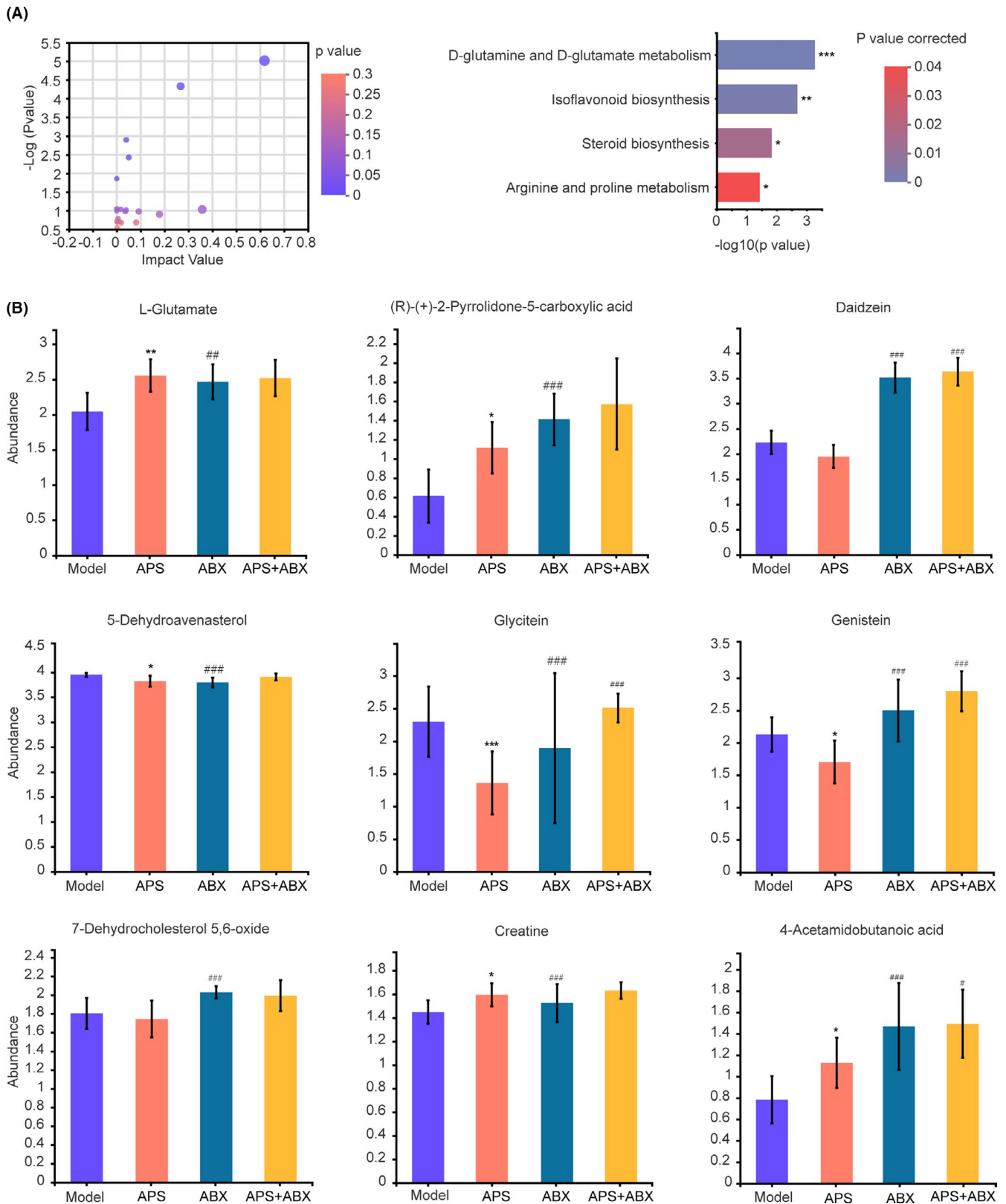


**FIGURE 6** *Astragalus polysaccharides* (APS) improve the metabolic function of gut microbiota. A, Pathway enrichment of differential metabolites in the APS group compared with the Model group. B, Comparison of the abundance of pathway-related metabolites in four groups. \* $P < .1$ ; \*\* $P < .05$ ; \*\*\* $P < .001$  compared with Model group. # $P < .1$ ; ## $P < .05$ ; ### $P < .001$  compared with APS group

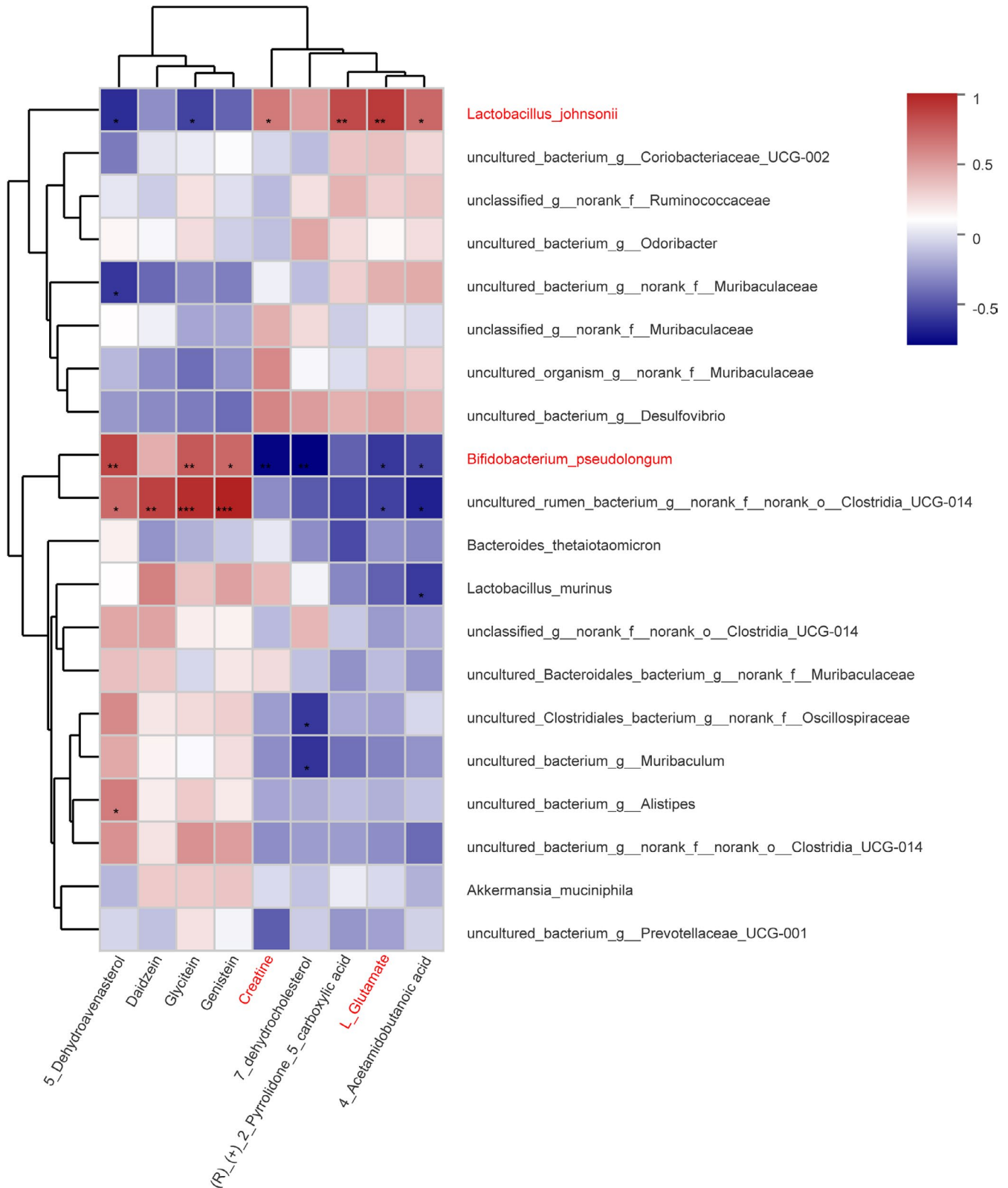


**FIGURE 7** Correlation between changes of abundance in fecal metabolites and gut microbiota. Nine fecal metabolites were selected. The heat map shows the Spearman correlation coefficient between changes in these metabolite concentrations and changes in relative abundance of species. The intensity of the colors represents the degree of positive or negative association. \* $P < .05$ , \*\* $P < .01$ , \*\*\* $P < .001$

However, here, most of these two metabolites in the APS group were downregulated compared with the other three groups. Therefore, it may not be through them that APS exert antitumor effects. In further

study, the role of metabolites L-glutamate and creatine in the treatment of melanoma and specific mechanisms will be further studied. Moreover, in this research, we just used the melanoma mouse model

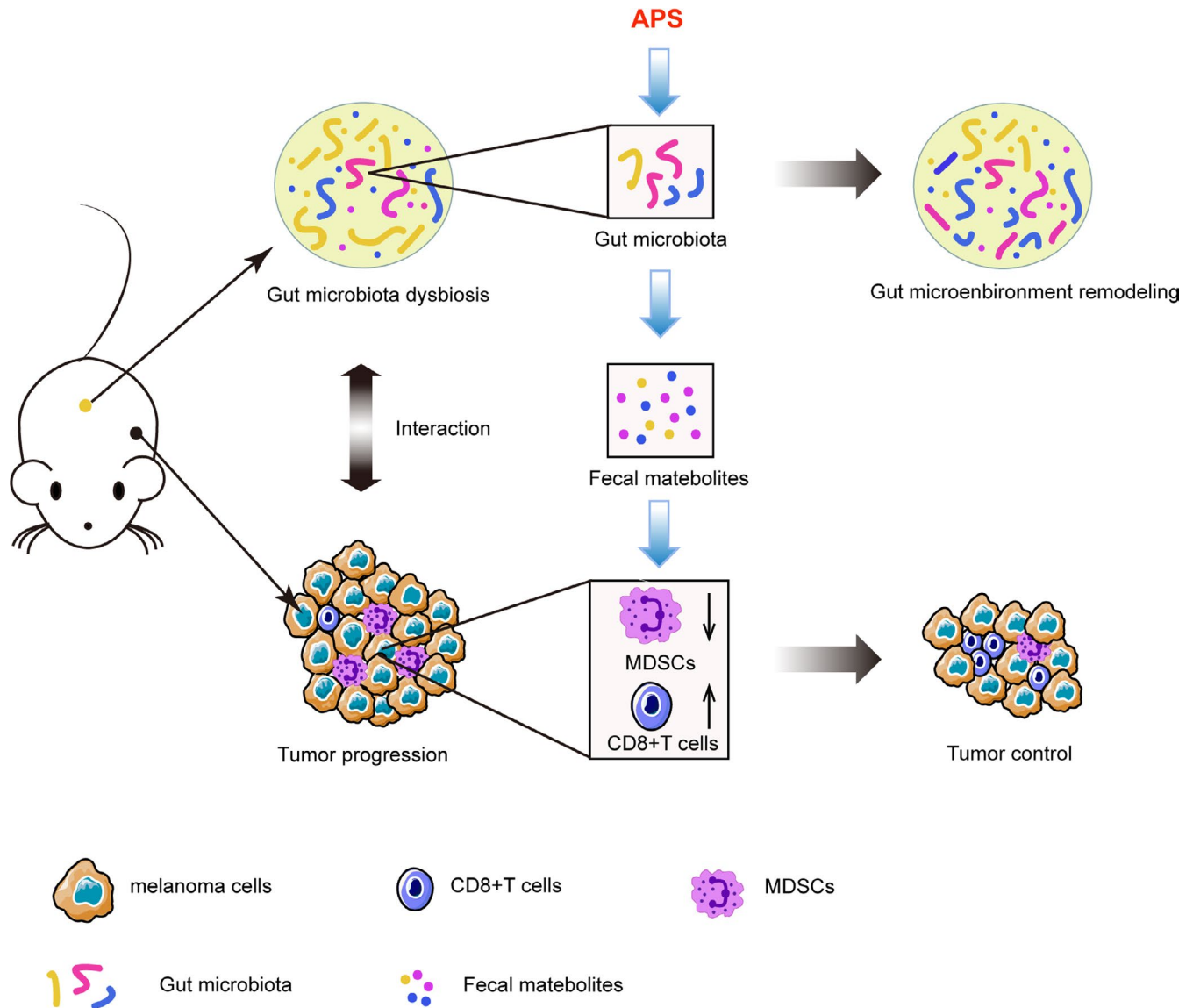


**FIGURE 8** Summary of the antitumor effect of *Astragalus polysaccharides* (APS) in melanoma model

to observe the changes in the gut and tumor microenvironment. We will further explore whether APS play an antitumor role in other tumors by regulating gut microbiota.

In conclusion, our study demonstrated that the antitumor effect of APS was related to its attenuation of the immunosuppressive activity of MDSC in melanoma-bearing mice, and this was dependent on the remodeling of gut microbiota and metabolic function (Figure 8). These findings indicated that APS has therapeutic potential and is of great significance to the modern application of traditional Chinese medicine.

#### ACKNOWLEDGMENTS

This work was supported by the National Natural Science Foundation of China [No.81973543]; the Shanghai Science and Technology Action Innovation Plan [No.19401901600]; and the Education and Scientific Research Projects of 2021 in the 14th Five Year Plan of National Higher Education of Traditional Chinese Medicine [No. YB-20-08].

#### DISCLOSURE

The authors have no conflict of interest.

#### ORCID

Guiqing Ding  <https://orcid.org/0000-0003-1612-9506>

#### REFERENCES

- Bray F, Ferlay J, Soerjomataram I, Siegel RL, Torre LA, Jemal A. Global cancer statistics 2018: GLOBOCAN estimates of incidence and mortality worldwide for 36 cancers in 185 countries. *CA Cancer J Clin*. 2018;68:394-424.
- Lodde G, Zimmer L, Livingstone E, Schadendorf D, Ugurel S. Malignant melanoma. *Hautarzt*. 2020;71:63-77.
- Tuccitto A, Shahaj E, Vergani E, et al. Immunosuppressive circuits in tumor microenvironment and their influence on cancer treatment efficacy. *Virchows Arch*. 2019;474:407-420.
- Dysthe M, Parihar R. Myeloid-derived suppressor cells in the tumor microenvironment. *Adv Exp Med Biol*. 2020;1224:117-140.

5. Jiang H, Gebhardt C, Umansky L, et al. Elevated chronic inflammatory factors and myeloid-derived suppressor cells indicate poor prognosis in advanced melanoma patients. *Int J Cancer*. 2015;136:2352-2360.
6. Gopalakrishnan V, Spencer CN, Nezi L, et al. Gut microbiome modulates response to anti-PD-1 immunotherapy in melanoma patients. *Science*. 2018;359:97-103.
7. Sepich-Poore GD, Zitvogel L, Straussman R, Hasty J, Wargo JA, Knight R. The microbiome and human cancer. *Science*. 2021;371:eabc4552.
8. Sivan A, Corrales L, Hubert N, et al. Commensal bifidobacterium promotes antitumor immunity and facilitates anti-PD-L1 efficacy. *Science*. 2015;350:1084-1089.
9. Xu C, Ruan B, Jiang Y, et al. Antibiotics-induced gut microbiota dysbiosis promotes tumor initiation via affecting APC-Th1 development in mice. *Biochem Biophys Res Commun*. 2017;488:418-424.
10. Jenkins SV, Robeson MS 2nd, Griffin RJ, et al. Gastrointestinal tract dysbiosis enhances distal tumor progression through suppression of leukocyte trafficking. *Cancer Res*. 2019;79:5999-6009.
11. Li Y, Tinoco R, Elmén L, et al. Gut microbiota dependent antitumor immunity restricts melanoma growth in Rnf5(-/-) mice. *Nat Commun*. 2019;10:1492.
12. Dong M, Meng Z, Kuerban K, et al. Diosgenin promotes antitumor immunity and PD-1 antibody efficacy against melanoma by regulating intestinal microbiota. *Cell Death Dis*. 2018;9:1039.
13. Rutkowski MR, Stephen TL, Svoronos N, et al. Microbially driven TLR5-dependent signaling governs distal malignant progression through tumor-promoting inflammation. *Cancer Cell*. 2015;27:27-40.
14. Ge Y, Ahmed S, Yao W, You L, Zheng J, Hileuskaya K. Regulation effects of indigestible dietary polysaccharides on intestinal microflora: an overview. *J Food Biochem*. 2021;45:e13564.
15. Cui F, Shi CL, Zhou XJ, et al. Lycium barbarum polysaccharide extracted from lycium barbarum leaves ameliorates asthma in mice by reducing inflammation and modulating gut microbiota. *J Med Food*. 2020;23:699-710.
16. Liu J, Yu J, Peng X. Poria cocos polysaccharides alleviates chronic nonbacterial prostatitis by preventing oxidative stress, regulating hormone production, modifying gut microbiota, and remodeling the DNA methylome. *J Agric Food Chem*. 2020;68:12661-12670.
17. Wang RJ, Wang JY, Zhang TT, Cheng XD. Regulation of astragalus polysaccharides on the expression of PD-1/PD-Ls in melanoma mice. *J Shanghai Univ Chin Med*. 2014;28:74-79.
18. [https://iacuc.ucsf.edu/sites/g/files/tksra751/f/wysiwyg/GUIDE LINE%20-Tumor%20Induction%20in%20mice%20and%20rats](https://iacuc.ucsf.edu/sites/g/files/tksra751/f/wysiwyg/GUIDE%20LINE%20-Tumor%20Induction%20in%20mice%20and%20rats)
19. Hill DA, Hoffmann C, Abt MC, et al. Metagenomic analyses reveal antibiotic-induced temporal and spatial changes in intestinal microbiota with associated alterations in immune cell homeostasis. *Mucosal Immunol*. 2010;3:148-158.
20. Chang CJ, Lin CS, Lu CC, et al. Ganoderma lucidum reduces obesity in mice by modulating the composition of the gut microbiota. *Nat Commun*. 2015;6:7489.
21. Tobin RP, Jordan KR, Kapoor P, et al. IL-6 and IL-8 are linked with myeloid-derived suppressor cell accumulation and correlate with poor clinical outcomes in melanoma patients. *Front Oncol*. 2019;9:1223.
22. Auyeung KK, Han QB, Ko JK. Astragalus membranaceus: a review of its protection against inflammation and gastrointestinal cancers. *Am J Chin Med*. 2016;44:1-22.
23. Ma XQ, Shi Q, Duan JA, Dong TT, Tsim KW. Chemical analysis of radix astragalii (Huangqi) in China: a comparison with its adulterants and seasonal variations. *J Agric Food Chem*. 2002;50:4861-4866.
24. Zheng Y, Ren W, Zhang L, Zhang Y, Liu D, Liu Y. A review of the pharmacological action of astragalus polysaccharide. *Front Pharmacol*. 2020;11:349.
25. Li BH, Garstka MA, Li ZF. Chemokines and their receptors promoting the recruitment of myeloid-derived suppressor cells into the tumor. *Mol Immunol*. 2020;117:201-215.
26. Gabrilovich DI, Nagaraj S. Myeloid-derived suppressor cells as regulators of the immune system. *Nat Rev Immunol*. 2009;9:162-174.
27. Chattopadhyay I, Dhar R, Pethusamy K, et al. Exploring the role of gut microbiome in colon cancer. *Appl Biochem Biotechnol*. 2021;193:1780-1799.
28. Iida N, Dzutsev A, Stewart CA, et al. Commensal bacteria control cancer response to therapy by modulating the tumor microenvironment. *Science*. 2013;342:967-970.
29. Vaziri F, Colquhoun S, Wan YY. Hepatocellular carcinoma immunotherapy: the impact of epigenetic drugs and the gut microbiome. *Liver Res*. 2020;4:191-198.
30. Qiu M, Huang K, Liu Y, et al. Modulation of intestinal microbiota by glycyrrhizic acid prevents high-fat diet-enhanced pre-metastatic niche formation and metastasis. *Mucosal Immunol*. 2019;12:945-957.
31. Tang S, Liu W, Zhao Q, et al. Combination of polysaccharides from *Astragalus membranaceus* and *Codonopsis pilosula* ameliorated mice colitis and underlying mechanisms. *J Ethnopharmacol*. 2021;264:113280.
32. Li B, Hong Y & Gu Y et al. Functional metabolomics reveals that astragalus polysaccharides improve lipids metabolism through microbial metabolite 2-hydroxybutyric acid in obese mice. 2020. <https://doi.org/10.1016/j.eng.2020.05.023>.
33. Lv J, Zhang Y, Tian Z, et al. Astragalus polysaccharides protect against dextran sulfate sodium-induced colitis by inhibiting NF- $\kappa$ B activation. *Int J Biol Macromol*. 2017;98:723-729.
34. Lu J, Chen X, Zhang Y, et al. Astragalus polysaccharide induces anti-inflammatory effects dependent on AMPK activity in palmitate-treated RAW264.7 cells. *Int J Mol Med*. 2013;31:1463-1470.
35. Sonoda A, Kamiyama N, Ozaka S, et al. Oral administration of antibiotics results in fecal occult bleeding due to metabolic disorders and defective proliferation of the gut epithelial cell in mice. *Genes Cells*. 2018;23:1043-1055.
36. Pushalkar S, Hundeyin M, Daley D, et al. The pancreatic cancer microbiome promotes oncogenesis by induction of innate and adaptive immune suppression. *Cancer Discov*. 2018;8:403-416.
37. Peng M, Lee SH, Rahaman SO, Biswas D. Dietary probiotic and metabolites improve intestinal homeostasis and prevent colorectal cancer. *Food Funct*. 2020;11:10724-10735.
38. Chen SM, Chieng WW, Huang SW, Hsu LJ, Jan MS. The synergistic tumor growth-inhibitory effect of probiotic lactobacillus on transgenic mouse model of pancreatic cancer treated with gemcitabine. *Sci Rep*. 2020;10:20319.
39. Ghanavati R, Akbari A, Mohammadi F, et al. Lactobacillus species inhibitory effect on colorectal cancer progression through modulating the Wnt/ $\beta$ -catenin signaling pathway. *Mol Cell Biochem*. 2020;470:1-13.
40. Mager LF, Burkhard R, Pett N, et al. Microbiome-derived inosine modulates response to checkpoint inhibitor immunotherapy. *Science*. 2020;369:1481-1489.
41. Zagato E, Pozzi C, Bertocchi A, et al. Endogenous murine microbiota member faecalibaculum rodentium and its human homologue protect from intestinal tumour growth. *Nat Microbiol*. 2020;5:511-524.
42. Tanoue T, Morita S, Plichta DR, et al. A defined commensal consortium elicits CD8 T cells and anti-cancer immunity. *Nature*. 2019;565:600-605.
43. Thirunavukkarasan M, Wang C, Rao A, et al. Short-chain fatty acid receptors inhibit invasive phenotypes in breast cancer cells. *PLoS One*. 2017;12:e0186334.
44. Ma C, Han M, Heinrich B, et al. Gut microbiome-mediated bile acid metabolism regulates liver cancer via NKT cells. *Science*. 2018;360:eaan5931.

45. Kaufmann Y, Klimberg VS. Effect of glutamine on gut glutathione fractional release in the implanted tumor model. *Nutr Cancer*. 2007;59:199-206.
46. Deminice R, Cella PS, Padilha CS, et al. Creatine supplementation prevents hyperhomocysteinemia, oxidative stress and cancer-induced cachexia progression in Walker-256 tumor-bearing rats. *Amino Acids*. 2016;48:2015-2024.
47. Campos-Ferraz PL, Gualano B, das Neves W, et al. Exploratory studies of the potential anti-cancer effects of creatine. *Amino Acids*. 2016;48:1993-2001.
48. Cella PS, Marinello PC, Borges FH, et al. Creatine supplementation in Walker-256 tumor-bearing rats prevents skeletal muscle atrophy by attenuating systemic inflammation and protein degradation signaling. *Eur J Nutr*. 2020;59:661-669.
49. Di Biase S, Ma X, Wang X, et al. Creatine uptake regulates CD8 T cell antitumor immunity. *J Exp Med*. 2019;216:2869-2882.
50. Chu H, Li J, Liu T, Miao N, Zhang W. Anticancer effects of Daidzein against the human melanoma cell lines involves cell cycle arrest, autophagy and deactivation of PI3K/AKT signalling pathways. *J BUON*. 2020;25:485-490.
51. Erten F, Yenice E, Orhan C, et al. Genistein suppresses the inflammation and GSK-3 pathway in an animal model of spontaneous ovarian cancer. *Turk J Med Sci*. 2021;51:1465-1471.

**How to cite this article:** Ding G, Gong Q, Ma J, Liu X, Wang Y, Cheng X. Immunosuppressive activity is attenuated by *Astragalus polysaccharides* through remodeling the gut microenvironment in melanoma mice. *Cancer Sci*. 2021;112:4050-4063. <https://doi.org/10.1111/cas.15078>